Energy Transfer Process and Process Gas Flow Model in Nitric Acid Production

Fadime Menekşe İkbal [1] , Oğuzhan Erbaş [1*] , Özer AYDIN[1]

[1] *Dumlupınar University Graduate Education Institute, Department of Mechanical Engineering, Kutahya, Turkey*

ABSTRACT

In the Oswald process, ammonia is reacted with oxygen under the catalyst of platinum to form oxides, which are converted into acid. Acid nitriding processes are essential in industry, and many kinds of products, such as plastics, paints, and explosives, are obtained this way. Achieving energy savings and improving production reflexes by monitoring energy consumption on a process basis in such enterprises requires defining the current process flows and structure through a model and analyzing them with parameter changes. In this study, the energy transfer process of NO_x gases obtained in the ammonia oxidation reactor and used as process gas in a nitric acid production facility and the parameters affecting the process were investigated. The parameters affecting the efficiency were determined. The problems were addressed by considering the energy efficiency of the facility. The ammonia oxidation reactor is the most essential part of the system. For this reason, the operating parameters of the old reactors in the facility were compared with the revised new reactors. After the revision, the efficiency and performance of the system were examined in old and new reactors. In addition, the flow and hydrodynamic structure of the existing process gas in the new reactors were reviewed with the ANSYS Fluent program, that is, CFD analysis.

Keywords: Nitric Acid Production Process; Ammonia Oxidation Reactor; Process Gas; Flow Model

Nitrik Asit Üretiminde Enerji Aktarım Süreci ve Proses Gazı Akış Modeli

ÖZ

Ostwald prosesinde, platin katalizörlüğünde amonyak, oksijenle reaksiyona sokularak oksitler meydana getirilir ve bunlar da aside dönüştürülür. Asitle yapılan nitrolama prosesleri endüstride önemli olup, bu yolla plastikler, boyalar ve patlayıcı maddeler gibi pek çok çeşit ürün elde edilir. Bu tür işletmelerde prosesler bazında enerji tüketiminin izlenmesiyle enerji tasarrufu sağlanması ve üretim reflekslerinin geliştirilmesi, mevcut proses akışlarının ve yapısının bir model üzerinden tanımlanarak, parametre değişimleri ile analizini gerektirmektedir. Bu çalışmada, bir nitrik asit üretim tesisinde amonyak oksidasyon reaktöründe elde edilen ve proses gazı olarak kullanılan NOx gazlarının enerji aktarım süreci ile prosesi etkileyen parametrelerin araştırılması yapılmış olup, verimliliği etkileyen parametreler belirlenmiştir. Tesisin enerji verimliliği göz önüne alınarak problemler ele alınmıştır. Amonyak oksidasyon reaktörü sistemin en önemli kısmıdır. Bu

*Corresponding Author: Oğuzhan ERBAŞ
oguzhan.erbas@dpu.edu.tr

nedenle tesisteki eski reaktörlerin işletme parametreleri ile yerine revize edilen yeni reaktörlerin karşılaştırılması yapılmıştır. Revizyon sonrası eski ve yeni reaktörlerde sistemin verimliliği ile performansı incelenmiştir. Ayrıca yeni reaktörlerde mevcut proses gazının akışı ve hidrodinamik yapısı ANSYS Fluent programı yani CFD analizi ile incelenmiştir.

Anahtar Kelimeler: Nitrik Asit Üretim Prosesi; Amonyak Oksidasyon Reaktörü; Proses Gazı; Akış Modeli

Corresponding Author: Oğuzhan ERBAŞ
oguzhan.erbas@dpu.edu.tr

1. INTRODUCTION

The earliest history of nitric acid dates back to the 14th century. At that time, royal water [1] (*aqua*), a solution that could dissolve gold and platinum regia) was used to produce. Under the influence of the First Industrial Revolution, Nitric Acid was produced from atmospheric air for industrial use in 1905 by the ¨Birkeland – Eyde" process [2]. It was built in 1913 with the "Haber- Bosch" process [3]; it is the leading industrial method used today for the production of ammonia.

The history of ammonia synthesis began at the beginning of this century when Haber and Bosch realized the economical production of hydrogen for the first time and the production of NH3 directly from hydrogen and nitrogen. The Haber- Bosch process was discovered by German chemists Fritz Haber and Carl Bosch in the 20th century.

Converts hydrogen (H2) and atmospheric nitrogen (N2) into ammonia (NH3) by using a metal catalyst under high temperatures and pressures. Although the Haber-Bosh process is used today mainly to produce fertilizer, during World War I, it was used as a source of ammonia for making explosives.

Chernyshev et al . studied the improvement process for the ammonia oxidation reaction. They have made improvements because the commissioning process in a nitric acid plant is one of the most critical stages in terms of safety and platinum loss in the entire ammonia oxidation process [4].

Chuah et al . demonstrated the design aspects of a shallow-bed reactor involving a swift, diffusion-controlled reaction. Methods for estimating the catalyst bed's mesh count, diameter, height, and volume are discussed [5].

Bartosz et al. described the effect of various design changes of the ammonia oxidation reactor in the nitric acid plant on the flow distribution of the air-ammonia mixture. CFD (computational fluid dynamics) simulations of turbulent flow were performed with the SST k-ω turbulence model to close the RANS (Reynolds Averaged Navier-Stokes) system of equations [6].

Husaini et al ., a primary waste heat boiler (WHB) at an ammonia plant, experienced cap leakage and outer tube rupture ten months after the last repair and replacement. Therefore, Primary WHB examined the external pipe failure cap leak improvement [7].

Hamad et al. observed repeated failures in the outlet region of the superheater tube integrated into a waste heat boiler thermally coupled to an ammonia oxidation reactor. The primary root cause of repeated failures of superheater tubes is short-term overheating after rapid cooling of the lines due to the sudden stop of steam flow inside the connecting lines in case of shutdown of the unit, reducing the thermal resistance of the lines [8].

Hamed et al. simulated the flow distribution within a Monica oxidation reactor using Computational Fluid Dynamics (CFD) code. CFD results showed that the flow was unevenly distributed within the reactor due to the improper header design of the reactor [9].

The literature on nitric acid production facilities includes the importance of the ammonia oxidation reactor, catalyst selection, use, and properties, and NO_x released into the environment in nitric acid production. Strategies to reduce emissions and the importance of filtration are emphasized. Energy efficiency is also among the critical issues. For this, facility size, selection of machinery and equipment, heat utilization, stack emissions, and operating costs are among the essential factors.

The aim is to determine the heat transfer and pressure losses in the waste heat boiler of the ammonia oxidation reactor using the flow model. It is a challenge to find an analytical solution for this. The energy equations and turbulence models were solved using the ANSYS Fluent Analysis program. In a simplified approach, heat transfer and radiation from the outer body to the outside are neglected. The geometry was drawn with simple lines to obtain an analytical solution. Therefore, three-dimensional data was used under the specified boundary conditions.

In this study, the factors affecting the process efficiency of the nitric acid production facility were investigated, and the parameters affecting the efficiency were determined. The problems were addressed by considering the energy efficiency of the facility. The ammonia oxidation reactor is the most essential part of the system. For this reason, the old reactors in the facility were examined and compared with the newly revised reactors. After the revision, the efficiency and performance of the system were reviewed in old and new reactors. The flow and hydrodynamic structure of the new reactors were examined with CFD analysis of the ANSYS Fluent program. Compared with facility data. As a result, the facility data and numerical results were similar.

2. ENERGY TRANSFER PROCESS IN NITRIC ACID PRODUCTION

Nitric acid (HNO_3) is a vital mineral that is clear, colorless, and caustic. It is used in industry in the production of fertilizers and explosives. The basic nutrients that play an important role in the fertilizer industry are nitrogen (N), phosphorus (P), and potassium (K). are sorted. The fertilizer to be produced depends on the nutrient to be used in the fertilizer production plants. It can be nitrogen, phosphorus, potassium, or complex fertilizer. Ammonia (NH_3), nitric acid (HNO_3), sulphuric acid (H_2SO_4), and phosphoric acid (H_3PO_4) are important industrial chemicals and, although used in industry, are mainly used in fertilizer production. The energy required in some fertilizer production plants comes from the plant's power stations. is met. For this reason, only the plants in the production phase are considered in assessing

such plants. Not only the plants but also the plants that supply energy should be considered. The physical and chemical properties of nitric acid are given in Table 1.

Table 1: Physical and chemical properties of nitric acid [10]

Nitric acid	55%
Water	45%
Appearance	Colorless, yellowish liquid
Smell	Sultry, sharp
Solubility in Water	Completely soluble
Density 20 °C	1,339 (55%)
pH	< 1.0
Boiling point	103.4 °C (20%)
	120.4 °C (60%)
Freezing point	-17 °C (20%)
	-22.4 °C (60%)
Vapor Density	2
Vapor Pressure 20 °C	0.77kPa (60%)
Iron (ppm)	0.02
Chloride (ppm)	Maximum 5

The process is given in Figure 1 to improve environmental quality based on sustainability and volunteering, a business needs to know the consequences of its activities and the resulting environmental impacts. Environmental indicators express the resources consumed and the waste generated per unit product (kg, ton, etc.) produced in a business. These indicators are also called specific consumption or specific amounts of waste generated. Environmental indicators play an active role in businesses' ability to capture resource efficiency opportunities. By determining its environmental indicators, a business can see at which points it can make savings by implementing which practices. Wastewater, solid waste, and emissions generated during processes and other operational activities in the fertilizer industry are the main areas of impact.
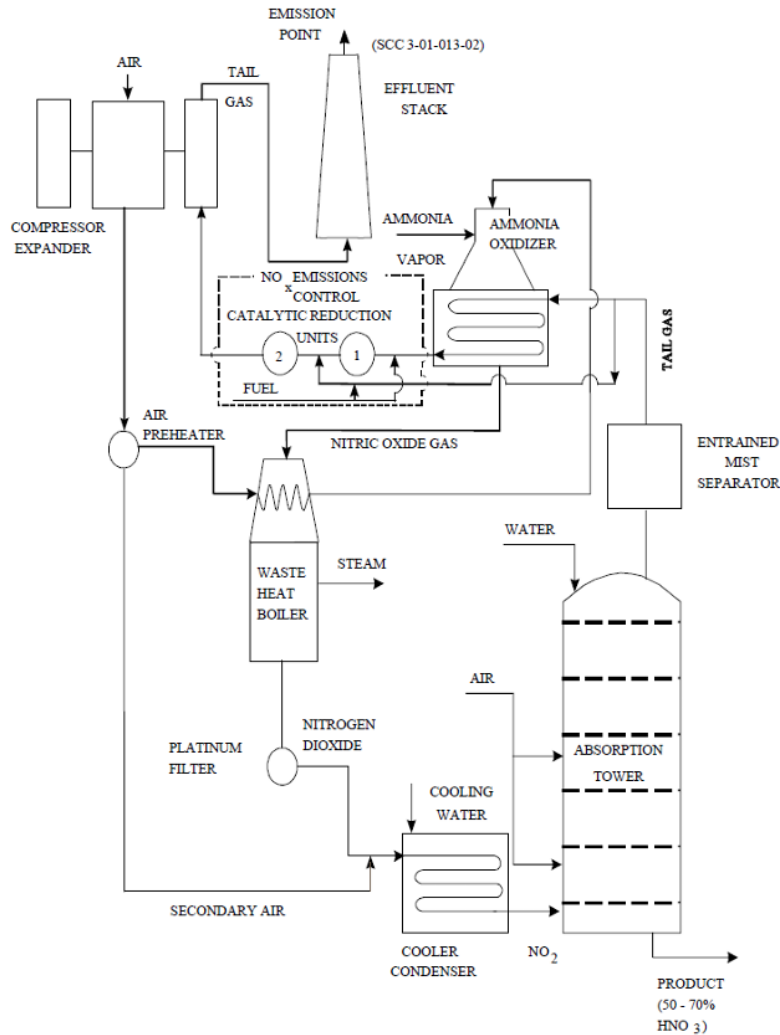
Figure 1: Nitric acid production process [11]

In the production of nitric acid, first, Ammonia is oxidized to obtain Nitric Oxide (Nitrogen Monoxide, NO), then NO is further oxidized to NO_2 (nitrogen dioxide). In the last stage, NO_2 gas is absorbed with water to obtain nitric acid (HNO_3). This cycle is called the Ostwald Process.

Nitric Acid Production Process Flow sequence is as follows [12]:

1. Filtration of entering air
2. Pressurization of air
3. Preparation of air/ammonia mixture
4. Catalytic ammonia oxidation (platinum/rhodium-based catalyst with a palladium braid to retain the catalyst, which subsequently evaporates)
5. Energy recovery and reheating of gases by utilizing reaction heat
6. Cooling of gases
7. Gas pressurization, energy recovery, and cooling processes (for dual pressure systems only)

8. Absorption of NO_2 gas to be converted into nitric acid

9. Flue gas (tail gas) heating

10. It generates electricity by operating a gas turbine by utilizing expansion while reducing the waste gases to atmospheric pressure.

3. MATERIALS AND METHODS

3.1. General Equations in Turbulent Flow

ANSYS Fluent software is a program for the numerical analysis of flow and heat problems. General equations that represent flow problems are called Navier-Stokes equations. The Navier-Stokes equation, which governs flow problems in its most general form, consists of the continuity equation, momentum equation, and energy equation [13].

3.1.1. Continuity Equation

For all flow regions, the fluent program solves the following continuity equation.

$$\frac{D\rho}{Dt} + \rho \nabla v = S_m \tag{1}$$

ρ; intensity, speed, S_m; is the mass added to the system (droplet, vapor, etc.), and t is time. In this study, $S_m=0$, and when three-dimensional, steady conditions are considered, time-dependent expressions are neglected.

$$\frac{\partial \rho}{\partial t} + \nabla(\rho \vec{V}) = 0 \tag{2}$$

The equation is written as (3), assuming the fluid density is constant.

$$\frac{\partial u}{\partial x} + \frac{\partial v}{\partial y} + \frac{\partial w}{\partial z} = 0 \tag{3}$$

3.1.2. Conservation of Momentum equation:

$$\frac{\partial}{\partial t}(\rho u_i) + \frac{\partial}{\partial x_j}(\rho u_i u_j) = -\frac{\partial P}{\partial x_i} + \frac{\partial \tau_{ij}}{\partial x_j} + \rho g_i + F_i \tag{4}$$

P; pressure, τ_{ij}; stress tensor, ρg_i; _gravitational force and F $_i$; It represents external forces.

(i indicates the direction of flow.)

The final form of three momentum equations in incompressible flow (5), (6), (7) is written as;

$$\rho \frac{Du}{Dt} = \rho g_x - \frac{\partial \rho}{\partial x} + \mu \nabla^2 u - p \left[\left(\frac{\overline{\partial u^2}}{\partial x} + \frac{\overline{\partial u'v'}}{\partial y} + \frac{\overline{\partial u'w'}}{\partial z} \right) \right], \tag{5}$$

$$\rho \frac{Dv}{Dt} = \rho g_y - \frac{\partial \rho}{\partial y} + \mu \nabla^2 v - p \left[\left(\frac{\overline{\partial u'v'}}{\partial x} + \frac{\overline{\partial v'^2}}{\partial y} + \frac{\overline{\partial v'w'}}{\partial z} \right) \right], \tag{6}$$

$$\rho \frac{DU}{Dt} = \rho g_x - \frac{\partial \rho}{\partial x} + \mu \nabla^2 u - p \left[\left(\frac{\overline{\partial u'w'}}{\partial x} + \frac{\partial v'w'}{\partial y} + \frac{\partial w'^2}{\partial z} \right) \right], \tag{7}$$

3.1.3. Energy Equation

$$\rho \frac{Dh}{Dt} - \frac{Dp}{Dt} = \emptyset - \nabla \dot{Q} \tag{8}$$

Here h = Enthalpy, Q = heat transfer, $\emptyset$= dissipation (loss function due to irreversible viscous work)[14].

h =e+ p/ρ $\qquad$ (9)

$\dot{Q}$=-k ∇T $\qquad$ (10)

$$\emptyset = \mu \left[2 \left(\frac{\partial u}{\partial x} \right)^2 + 2 \left(\frac{\partial v}{\partial y} \right)^2 + 2 \left(\frac{\partial w}{\partial z} \right)^2 + \left(\frac{\partial u}{\partial y} + \frac{\partial v}{\partial x} \right)^2 + \left(\frac{\partial v}{\partial z} + \frac{\partial w}{\partial y} \right)^2 + \left(\frac{\partial u}{\partial x} + \frac{\partial v}{\partial z} \right)^2 \right] - \frac{2}{3} \mu \left(\frac{\partial u}{\partial x} + \frac{\partial v}{\partial y} + \frac{\partial w}{\partial z} \right)^2 \tag{11}$$

3.2. Fluent Software Turbulence Models

Turbulence, middle and high Reynolds in numbers, in fluids observed 3D, is an unstable and irregular movement. Fluid movements generally involve low-viscosity fluids. Since it is based on almost all currents, it is turbulent. Turbulence is not a property of the liquid; the rough velocity field characterizes it. These turbulences are mixtures of transported quantities such as momentum, energy, and concentration. This study used the k-ω model, which is more suitable for fluids with high turbulence density; this model calculates scalable kinetic energy instead of kinetic energy.

3.2.1. k-ω Turbulence Model

An essential advantage of the k -ω formulation is the near wall calculation in low Reynolds number flows. This model is the complex required in the k-ε model. It does not need a non-linear damping function. Therefore, it gives more accurate and robust results. The k-ω model assumes that turbulent viscosity is related to turbulent kinetic energy and turbulence frequency [15].

$$\mu_t = \rho \frac{k}{\omega} \tag{12}$$

Beginning of the k -ω model by Wilcox Posted [16]. This model solves two transport equations, one for the turbulence kinetic energy, k, and the other for the turbulence frequency, w. The stress tensor is calculated according to the media-viscosity concept.

k equality;

$$\frac{\partial(\rho k)}{\partial t} + \nabla \cdot ((\rho U k) = \nabla \cdot \left[(\mu + \frac{\mu_t}{\sigma_k}) \nabla k \right] + P_k - \beta' \rho k \omega \tag{13}$$

ω Equality;

$$\frac{\partial(\rho \omega)}{\partial t} + \nabla \cdot (\rho U \omega) = \nabla \cdot \left[(\mu + \frac{\mu_t}{\sigma_\omega}) \nabla \omega \right] + a \frac{\omega}{k} P_k - \beta \rho \omega^2 \tag{14}$$

In addition to the independent variables, the density velocity vector is assumed to be known from the Navier-Stokes equation. P_k is the turbulence production amount calculated as in the k-ε model.

$$P_k = \mu_t \nabla U \cdot (\nabla U + \nabla U^\tau) - \frac{2}{3} \nabla \cdot U (3 \mu_T \nabla \cdot U + \rho k) + P_{kb} \tag{15}$$

Model constants β'=0.09, a=5/9, β=0.075, σ_k=2, σ_ω=2

Unknown Reynolds Stress Tensor is calculated from the following equation.

$$\tau_- = \mu_t \, 2 \, s - \rho \frac{2}{3} \, \delta_k \tag{16}$$

To avoid the reproduction of turbulence kinetic energies in stagnation zones, a limiter was applied to the production term by Menter [17]

$$\bar{P}_k = \min (P_k, C_{\lim} \epsilon) \tag{17}$$

3.3. Ammonia Oxidation Reactor Structure

The ammonia oxidation reactor consists of two parts: the combustion unit part (chemical reaction) and the waste heat boiler part that produces steam. The combustion unit part is shown in Figure 2, and the waste heat boiler with steam is shown in Figure 3.

Figure 2: Combustion unit section

Figure 3: Steam generating waste heat boiler

The oxidation reactor consists of three parts.

- Economizer (preheater): the part where the serpentine pipes are located.
- Evaporator (middle part): It is the part where pre-evaporation and evaporation occur.
- Superheater (upper part): This is the part where the superheaters are located.
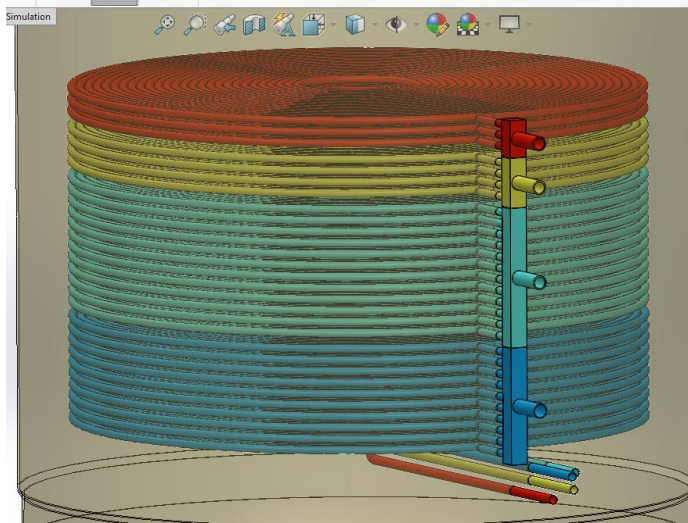
Figure 4: Steam generating waste heat boiler structure

The process process in ammonia oxidation reactors is as follows;

In ammonia reactors, it starts with the reaction of a compressed air + gas ammonia mixture on a platinum catalyst.

This chemical reaction is an exothermic reaction and as a result, heat and NO_x gases are released. (Reaction temperature is 850-900 ^0C).

The heat released is used to convert the water in the reactor into steam and to drive the turbine.

The turbine, driven by the steam it produces, turns the compressor and the compressed air required for combustion is obtained.

Thus, the system operates in a cycle that produces its own energy.

This study was conducted in three stages.

1. Stage: Ammonia oxidation reactor efficiency parameters were determined. A comparison was made between the old and new reactors.

2. Stage: Ammonia oxidation reactor mass and energy balance were checked.

3. Stage: Numerical analysis of the ammonia oxidation reactor was performed. The numerical analysis stages were as follows. First, in the first stage, the ammonia oxidation reactor was drawn in 3D with exact measurements in the Solidworks 2021 drawing program. In the second stage, 3D meshes were created in ANSYS Meshing to make the appropriate mesh structure. Digital analyzes ANSYS fluent Version It was implemented in 2020 R2. NO_x flowing from the reactor main body gas and water flow through the coils since it is turbulent, turbulence is used to get closer results. Model aspect realizable k-ω turbulence model was chosen. Detailed information about the software used and the models selected is available here. Are given in the section. In addition, assumptions made with the model geometry initial and boundary conditions in this chapter have been explained.

3.3.1. Revision Study

When the Nitric Acid Producing Facility was examined, it was seen that the reactor caused 90 % of the malfunctions. The reactors were renovated to eliminate these shutdowns and increase efficiency. The waste heat boiler (WHB) of the old reactors and the waste heat boiler (WHB) of the new reactor were examined in terms of efficiency, and the winding shape of the coils was designed differently. While the serpentines of the old reactor were square, most of the malfunctions were caused by the serpentines. The body of the new reactor is spirally arranged for optimum efficiency. No serpentine-related stops have occurred since the revision. As a result, Figure 5 and Figure 6, when examined, can be seen that the inlet and outlet temperatures in the new reactor have been improved.
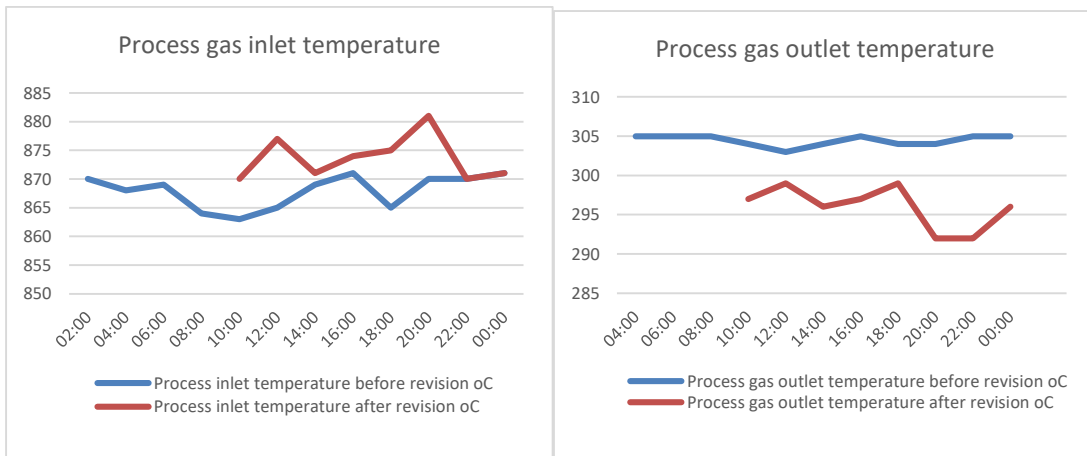

Figure 5: Changes in A and B reactor gas inlet and outlet temperatures
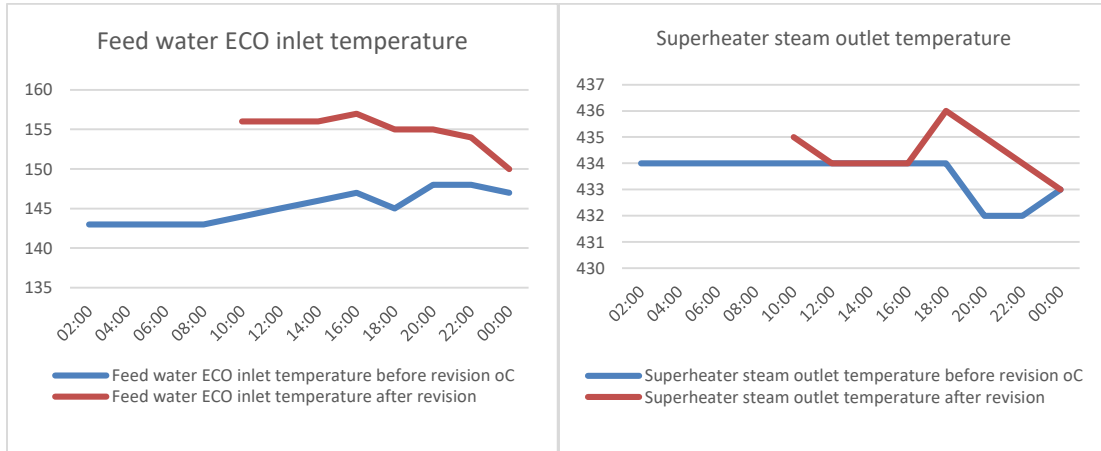
Figure 6: Changes in A and B reactor feed water ECO inlet and superheater steam outlet temperatures

With the renovation of the reactor, there was an increase hour in the amount of steam produced. There were no reactor-related malfunctions after the revision. Since there were no stoppages, production also increased. Since there was no stoppage due to the new changes, there was a 10 % increase in efficiency. Table 2 gives the operating parameters of the nitric acid plant before and after the reactor revision.

Table 2: Nitric acid plant operating parameters before and after reactor revision

	PRE-REVISION DATA	DATA AFTER REVISION
Sub platinum Temperature	865 - 870 ^{0}C	865 - 870 ^{0}C
NO gas output temperature	350 - 400 ^{0}C	250 - 310 ^{0}C
Superheated steam generation	33 t/h	36 t/h
Superheated steam temperature	410 ^{0}C	440 ^{0}C

3.3.2. Process Gas Flow Model

Under current operating conditions, the flow and hydrodynamic structure (velocity, temperature, and pressure distributions) of NO_x gas coming from the regions where the economizer, evaporator, and superheater coils are located were examined with the help of CFD analysis. The main structure of the analyzed reactor is shown in Figure 7. The reactor shown in Figure 7 was modeled 3D symmetrically from surface A, as shown below, with the help of the ANSYS- Space claim program, to examine the velocity, pressure, and temperature distributions of the waste gases formed after the reaction of 89 % air and 11 % NH$_3$.
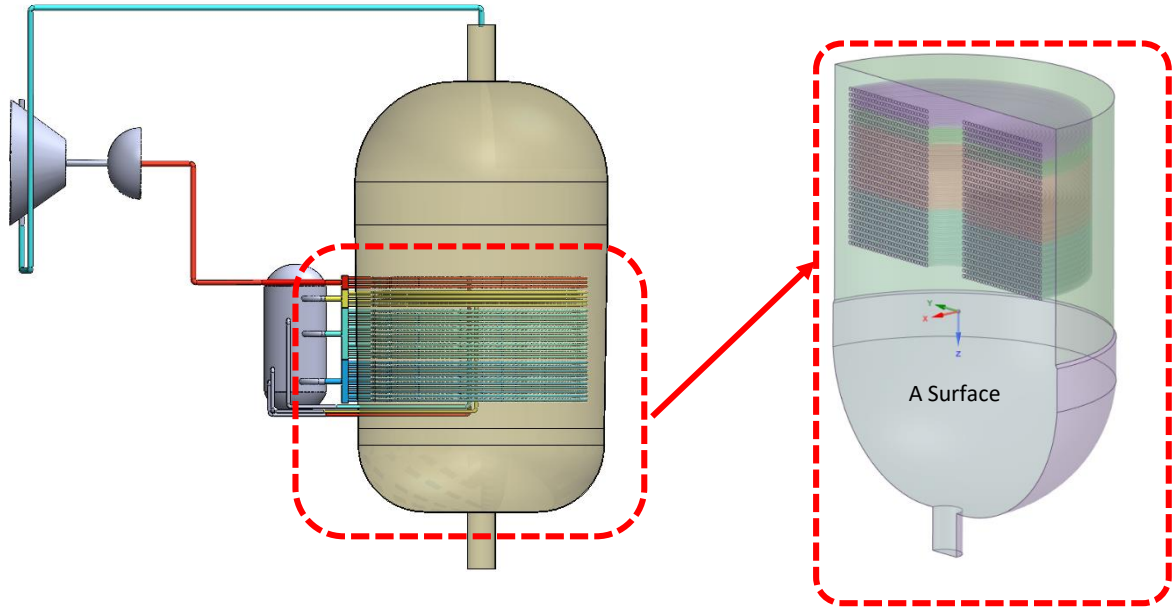
Figure 7: Ammonia oxidation reactor symmetric numerical model

The boundary conditions, gas properties, and material properties used for the analysis are also shown in Table 3.

Table 3: Inlet gas properties and material properties [18]

Characteristics of Inlet Gas		Material Properties	
Inlet Pressure	342,000 Pa	**Outer Body Material**	ST38.8
Input Speed	15 m/s	**Superheater Pipe Material**	13 CrMo4-5
Inlet Flow	51.525 Nm^3/h	**Vaporizer Pipe Material**	P235GH
Inlet Temperature	870 ^{0}C	**Pre-Evaporator Pipe Material**	P235GH
Exit gas combustion products	H_2O 16.35 Vol % N_2 68.25 Vol % NO 9.8 Vol% O_2 5.6 Vol %	**Economizer Pipe material**	SA213

With the help of Fluent software, Ansys simulations were carried out using the method and conservation equations below.

Table 4: Ansys fluent model parameters

Energy	Front		
Species Model	Species Transport Model- Mixture Material	**Options**	- Low -Re Correction - Viscous Heating -Curvature Correction -Production limiter -Buoyancy Effect (Full)
General	- Steady-state - Gravity (ten)		
Viscous Model	K- omega (2 equations)	**Material**	H_2O 16.35% N_2 68.25% NO 9.8% O_2 5.6%
K- omega Model	SST		

4. RESULTS

A reversible and exothermic reaction occurs between NH_3 and oxygen, producing process gas, i.e., nitrogen oxides (NO_x). Pressure and temperature values vary depending on the desired NO_x conversion rate. In addition, dilute and concentrated nitric acid production varies depending on the operating pressure of the process. In such enterprises, ensuring energy savings and improving production reflexes by monitoring energy consumption on a process basis requires defining the process flows and structure through a model and analyzing them with parameter changes. As shown in Figure 8, the reference plane is defined within the reactor to pass through the middle region of the system. The following section uses this reference plane to examine speed, pressure, and temperature contours.
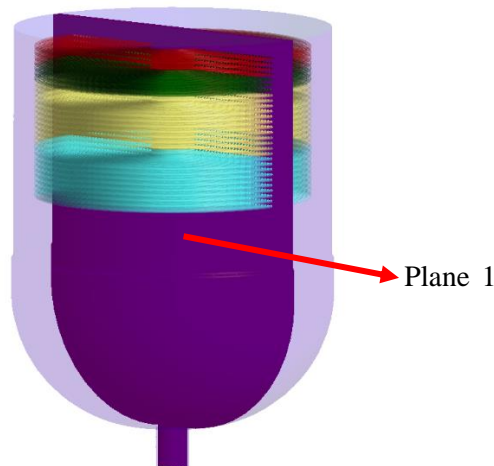

Figure 8: Reference plane (Plane 1)

The flow and hydrodynamic structure of the reaction mixture in the ammonia oxidation reactor were examined. CFD (computational fluid dynamics) simulation of turbulent flow looked at the velocity distribution. Figure 9 shows the analysis of velocity distribution contours obtained from ANSYS Fluent CFD. As a result of the study, the exit speed was obtained as 127 m/s. The rate increased due to the narrowing of the cross-section at the exit. The analysis model input and output parameter values are given in Table 5.
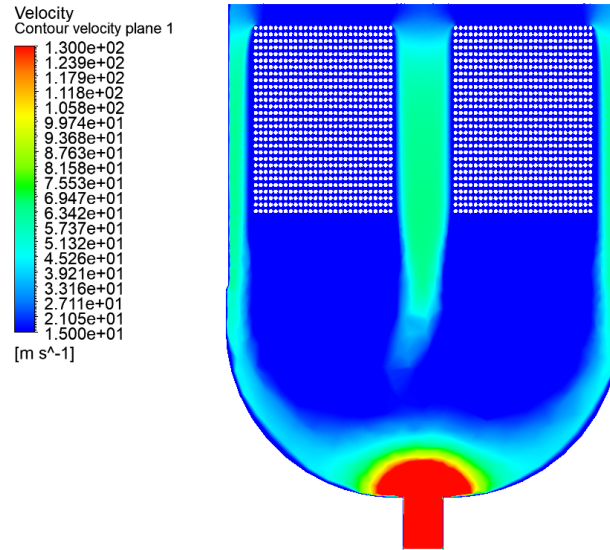

Figure 9: Velocity distribution obtained as a result of ANSYS Fluent CFD

Table 5: Analysis of model input and output values

Velocity (m/s)		Pressure (Pa)		Temperature (^{0}C)	
Inlet	Outlet	Inlet	Outlet	Inlet	Outlet
15	127	342000	237465	870	337

Figure 10 shows the temperature distribution contour analysis due to ANSYS Fluent CFD analysis. The temperature of the gas entering the system was determined as 870 ^{0}C, and the gas exit temperature was defined as 337 ^{0}C. This obtained value coincides with the facility data. The inlet pressure of the gas entering the system was defined as 342 kPa, and the outlet pressure of the gas was determined as 237.5 kPa. All values obtained were compatible.
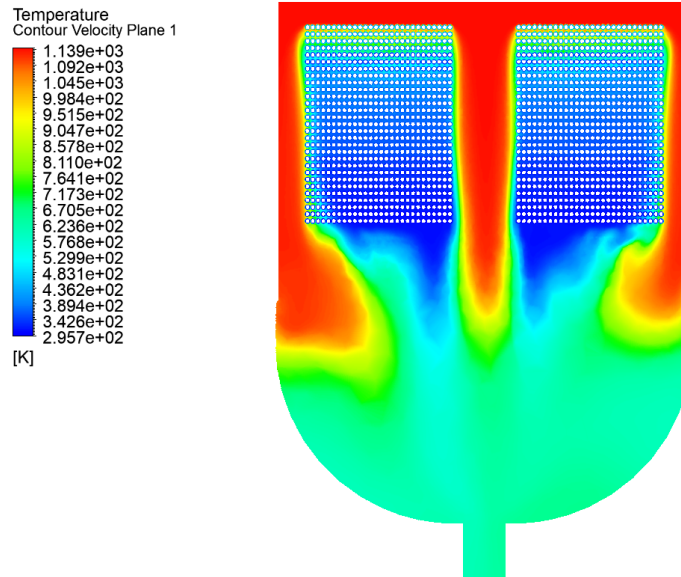
Figure 10: Temperature distribution obtained as a result of ANSYS Fluent CFD

5. CONCLUSIONS

In large industrial facilities, saving energy and improving production reflexes by monitoring energy consumption on a process basis requires defining the current process flows and structure through a model and analyzing them with parameter changes. In this study, the energy transfer process of NOx gases obtained in the ammonia oxidation reactor and used as process gas in a nitric acid production facility and the parameters affecting the process were investigated, and the parameters affecting the efficiency were determined. With the help of Computational Fluid Dynamics (CFD), detailed calculations were made and the flow field and other physical details were shown. The results of CFD analyses provide significant benefits in the simulation-based product design process, which helps simulate the operation of the product, and any problems, in the computer environment, and optimizes product performance.

CONFLICT OF INTEREST DECLARATION

There is no conflict of interest between the authors.

CONTRIBUTIONS OF THE AUTHORS

F.A.: Methodology, software, validation, investigation, resources, writing—original draft preparation.

S.A.: Methodology, validation, resources, editing.

T.A.: Methodology, software, validation.

REFERENCES

[1] Mellor, J. W. (1922). Supplement to Mellor's Comprehensive Treatise on Inorganic and Theoretical Chemistry: suppl. 3. K, Rb, Cs, Fr.Dary, G., (1913) *The Production of Nitrates by the Direct Electrolysis of Peat Deposits* , London Electrical Review, 73: 1020-1021.

[2] Modak, J. M. (2002). Haber process for ammonia synthesis. Resonance, 7(9), 69-77. Chernyshev, V. I., & Zjuzin, S. V. (2001). Improved start-up for the ammonia oxidation reaction. Platinum Metals Review, 45(1), 22-30.

[3] NurSulihatimarsyila A. W., Chuah T.G., Choong S. Y., Thayananthan.B (2005) *Estimation of Platinum Gauzes Catalyst for Ammonia Oxidation of Nitric Acid Production,* The Institution of Engineers, Malaysia Volume 66, Issue 4.

[4] Moszowski, B., Wajman, T., Sobczak, K., Inger, M., & Wilk, M. (2019). The analysis of distribution of the reaction mixture in ammonia oxidation reactor. *Polish Journal of Chemical Technology*, 21(1), 9-12.

[5] Ardy, H., Putra, Y. P., Anggoro, A. D., & Wibowo, A. (2021). Failure analysis of primary waste heat boiler tube in ammonia plant. *Heliyon*, 7(2).

[6] Abbasfard, H., Ghanbari, M., Ghasemi, A., Ghader, S., Rafsanjani, H. H., & Moradi, A. (2012). Failure analysis and modeling of super heater tubes of a waste heat boiler thermally coupled in ammonia oxidation reactor. *Engineering Failure Analysis*, 26, 285-292.

[7] Zanoni, M. A., Wang, J., & Gerhard, J. I. (2021). Understanding pressure changes in smouldering thermal porous media reactors. *Chemical Engineering Journal*, 412, 128642.

[8] Gemlik Gübre Sanayi A.Ş., (2003), Nitric Acid According to Safety*, Data Sheet* 91/155/EC

[9] Gabrielson, J. E. (1964). Potassium-nitrate from nitric acid and potassium-chloride. Iowa State University.

[10] National Research Council. (2004). *Air quality management in the United States*. National Academies Press.

[11] Yadav, A. S., Shukla, O. P., Sharma, A., & Khan, I. A. (2022). CFD analysis of heat transfer performance of ribbed solar air heater. Materials Today: *Proceedings*, 62, 1413-1419.

[12] Papa, F., Vaidyanathan, K., Keith, T. G., & DeWitt, K. J. (2000). Numerical computations of flow in rotating ducts with strong curvature. *International Journal of Numerical Methods for Heat & Fluid Flow,* 10(5), 541-557.

[13] Fluent Incorporated (1998). *FLUENT User's Guide.* Version 6.1,

[14] Suga, K. (2003). Predicting turbulence and heat transfer in 3-D curved ducts by near-wall second moment closures. *International Journal of Heat and Mass Transfer*, 46(1), 161-173.

[15] Lim, K. W., & Chung, M. K. (1999). Numerical investigation on the installation effects of electromagnetic flowmeter downstream of a 90 elbow–laminar flow case. *Flow Measurement and Instrumentation,* 10(3), 167-174.

[16] Heselton, P. E. (Ed.). (2020). *Boiler operator's handbook*. CRC Press.